THE DEVELOPMENT OF COMPRESSIVE STRENGTH, DRYING SHRINKAGE AND MICROSTRUCTURE OF FLY ASH GEOPOLYMER WITH FIELD PARA RUBBER LATEX

ABIDENG HAWA [1] * , WORAPHOT PRACHASAREE[2]
[1]*Department of Civil Engineering, Princess of Naradhiwas University, Narathiwat, Thailand 96000*
[2]*Department of Civil Engineering, Prince of Songkla University, Hat Yai, Songkhla Thailand 90112*

This study focused on the mechanical properties of fly ash geopolymer mortars with short heat curing and incorporating some field Para rubber latex (FPRL). The geopolymer mortar mixtures were prepared with fly ash to FPRL ratios 1:0.01, 1:0.025 and 1:0.05 by weight, and with varied heat curing times ranging from 0.5 to 4 h. The microstructure is investigated with scanning electron microscopy (SEM), but X-ray diffraction (XRD), and Fourier transform infrared spectroscopy (FTIR) analysis are used to obtain information about phase composition. The compressive strength and drying shrinkage were determined. The FPRL content of 1% and heat curing for 4 h gave the maximal compressive strengths after demolding and at 28 days, namely 47 and 61 MPa, respectively. SEM analysis indicated that the 1% FPRL geopolymer sample has a dense compact matrix with the low proportion of unreacted fly ash, which is likely associated with the high compressive strength.

Keywords: *geopolymer; field Para rubber latex; microstructure; drying shrinkage*

1. Introduction

Several parameters of geopolymerization have been studied in relation to mechanical properties, such as sodium silicate and aluminate contents, curing temperature, curing time, and addition of minerals. Generally, geopolymers are prepared with fly ash (FA) or metakaolin as the main raw material. However, the strength and physical properties can be improved by mineral admixtures or wastes from industrial processes. Ranjbar et al. [1,2] studied geopolymer mortars with fly ash and palm oil fuel ash. Increasing the palm oil fuel ash content in FA based geopolymer mortars decreased density of the mixture. Rice husk ash (RHA) used as a partial replacement in FA is beneficial to the strength development of geopolymers [3]. Meanwhile, the increasing of RHA content achieved a significant improvement on the waterproof property of geopolymer [4]. Xie et al. [5] reported that the combination of ground granulated blast furnace slag (GGBS) and FA can provide excellent workability and mechanical performance for the geopolymer concrete with recycled coarse aggregates. The maximum compressive strength was obtained from geopolymer paste at the GGBS replacement of 20% in FA [6]. Alomayri [7] showed that FA based gepolymer paste containing nano-Al_2O_3 increases mechanical properties. The FA-based geopolymer comcrete containing silica fume provided high strength [8]. Badanoiu et al. [9] reported that the mass losses of geopolymer with waste glass and FA had a stability in water. Several studies have focused on the effects of SiO_2/ Al_2O_3 molar ratio. The added minerals need to be finely ground for high reactivity. Moreover, finely ground minerals can act as filler.

The study [10] reported that geopolymer was prepared from fly ash with RHA and used sodium silicate and sodium hydroxide with alkali activator. The compressive strength of such geopolymer was maximal at RHA content of 35%. Liu et al. [11] used FA and palm oil fuel ash (POFA) as binder materials for lightweight geopolymer concrete with oil palm shell. They reported that the compressive strength of sample increased with POFA content up to 20%, after which adding more POFA reduced the strength. Temuujin et al. [12] suggested that the addition of calcium compounds as calcium oxide (CaO) and calcium hydroxide $Ca(OH)_2$ improves compressive strength of fly ash based geopolymer paste cured at ambient temperature. Chindaprasirt et al. [13] stated that fly ash and silica fume can be used as raw materials of geopolymer. The optimum silica fume content was 3.75% for maximal compressive strength. Silica fume can improve reactivity of the binder system. However, a high content of silica fume in the geopolymer matrix increased the SiO_2/Al_2O_3 ratio excessively and adversely affected the strength. In the part of geopolymer containing field Para rubber latex (FPRL) there are only few researches. However, in this research [14] made geopolymer containing FPRL in four alternative mixtures. The samples were prepared with heat curing at four experimental fly ash to FPRL ratios (1: 0, 1: 0. 10, 1: 0. 20, and 1:0.30 by weight). It was observed that high FPRL content (10-30%) in the geopolymer matrix reduced its compressive strength.

* Autor corespondent/*Corresponding author*,
E-mail: abideng.hawa@gmail.com

The field Para rubber latex, FPRL, contains 30-40 of rubber particles and also non-rubber components, such as sludge, proteins, some inorganic materials, and water. In 2018, Thailand had a rubber plantation area of 20.0 million raise (3.2 million hectares). The annual production is approximately 4.84 million tons of Para rubber [15]. In 2018 Thailand produced approximately 14 million tons of FPRL.

This study focuses on fly ash geopolymer with added FPRL. The amount of FPRL ranged up to 5% by weight of fly ash. We also tested the alternative heat curing times at 80 ºC for 0.5, 1, 2, or 4 h. The study aimed to analyze the effects on compressive strength and drying shrinkage, and to investigate the microstructure using XRD, FTIR, and SEM.

2. Experimental details and testing methods

2.1 Materials

The fly ash (FA) and field Para rubber latex (FPRL) were obtained from Mae Moh power plant from Lampang province in northern Thailand and from Narathiwat province in southern Thailand, respectively. The chemical compositions, physical characteristics and mineral compositions are shown in Table 1 and Figure 1, respectively. The chemical composition of FA was analyzed using X-ray fluorescence (XRF). The total amount of the major oxides (SiO_2, Al_2O_3 and Fe_2O_3) was 77.7% while the CaO content was 12.5%. The physical characteristics of FA are presented in Table 1. The mean particle size of FA was ~25 µm. Cumulative particle size distribution is presented to percent volume passing. The XRD patterns of FA are displayed in Figure 1. The mineral phases in the FA include anhydrite ($Ca(SO_4)$), quartz (SiO_2) and magnetite (Fe_3O_4). FTIR was used to identify the main functional groups of FA. Figure 2 presents the FTIR spectrum of FA. This spectrum has a very sharp peak at 3449 cm^{-1} corresponding to the stretching vibrations of O-H. Bands associated with Si-O and Si-O-T (Si or Al) stretching vibrations were found at 1101 and 1028 cm^{-1}, and the band at 461 cm^{-1} was associated with Si-O stretching vibrations.

Field Para rubber latex (from rubber tree clonal variety RRIM 600) used in this study was collected from Narathiwat province in Thailand. The FPRL is a suspension with 35-40% total solid content. The particle size distribution of FPRL is in the range 0.04-4.0 µm.

The alkaline activators of geopolymerization reactions were prepared of sodium silicate (Na_2O = 14.85%, SiO_2 = 29.45% and H_2O = 55.7%), sodium hydroxide (NaOH) flakes of 99% purity, and water. Natural river sand passing through ASTM sieve No. 4, with particle size below 4.75 mm, the specific gravity of 2.56, and the fineness modulus of 2.59, was used to prepare geopolymer mortars.

2.2 Mixture proportions and curing of samples

The geopolymer samples were prepared by mixing of fly ash, river sand, sodium silicate, sodium hydroxide and water in proportions according to an experimental design. Field Para rubber latex was added as a stabilizing material. The mixture proportions are shown in Table 2. They were selected to maximize the compressive strength based on this test. The proportions of ash and alkaline activator were fixed, to assess the robustness of formulation. The samples were prepared in two steps. First, the fly ash and river sand were mixed for 3 minutes. Second, the sodium silicate, sodium hydroxide, and water were mixed to a homogeneous alkaline solution. Subsequently, the homogeneous alkaline solution was added to and mixed with the fly ash and river sand from the first step, for 3 minutes. Finally, to the mortar samples FPRL was added and mixed for 5 minutes. The fresh mortar was poured into acrylic molds and wrapped with polyvinyl, and cured at 80 ºC for 0.5, 1, 2, and 4 h. After heat curing, the samples were demolded and stored at ambient temperature until testing for compressive strength and drying shrinkage.

Table 1

The chemical composition and physical characteristics of fly ash.

Component	SiO_2	Al_2O_3	Fe_2O_3	CaO	SO_3	K_2O	MgO	Na_2O	TiO_2
%by weight	45.3	23.0	9.4	12.5	2.7	2.3	1.7	1.0	0.4
Volume	Mean particle size				<10%	<25%	<50%	<75%	<90%
µm	25.78				5.02	11.05	22.77	38.85	51.08

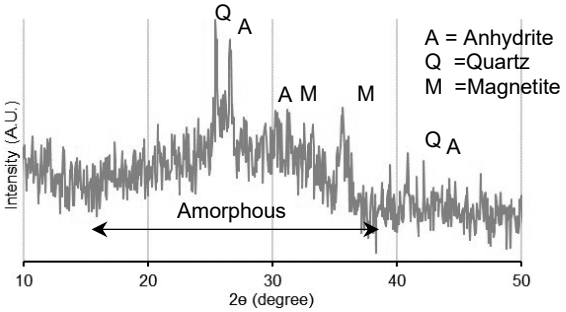

Fig. 1 – XRD pattern of FA.

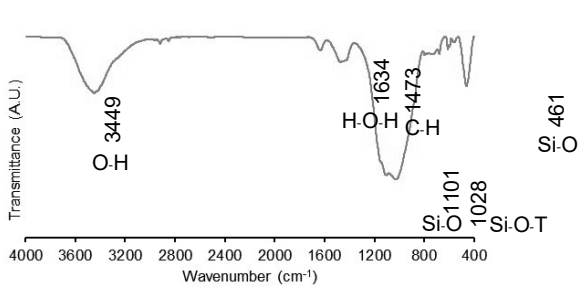

Fig. 2 – FT-IR spectrum of FA.

Table 2

Mixture proportions of the geopolymer samples (wt%.)

Mixture	SS	SH	W	FA	FPRL	RS	Heat curing (h)
F-0.5	5.46	3.64	5.68	22.72	0	62.5	0.5 (30 min)
1L-0.5					0.23		
2.5L-0.5					0.57		
5L-0.5					1.14		
F-1	5.46	3.64	5.68	22.72	0	625	1
1L-1					0.23		
2.5L-1					0.57		
5L-1					1.14		
F-2	5.46	3.64	5.68	22.72	0	625	2
1L-2					0.23		
2.5L-2					0.57		
5L-2					1.14		
F-4	5.46	3.64	5.68	22.72	0	625	4
1L-4					0.23		
2.5L-4					0.57		
5L-4					1.14		

Abbreviations used : SS = sodium silicate; SH = sodium hydroxide; W = water; FA = fly ash; FPRL = field Para rubber latex; RS = river sand In first column : F = Fly ash only, 1L = 1% FPRL. 2.5L = 2.5% FPRL, 5L = 5% FPRL

2.3 Methods

2.3.1 Compressive strength test

The geopolymer mortars were tested for compressive strength, after curing for 0.5, 1, 2 and 4 h 80 ◦C. The test was performed on 50x50x50 mm cubic at 0, 1, 7, and 28 days of age using an automatic compression tester machine. The compressive strength test was determined according to ASTM C109/C109M [16].

2.3.2 X-ray diffraction (XRD) analysis

XRD patterns of geopolymer paste were analyzed using an X'Pert MPD X-ray diffractometer (PHILIPS) for angles from 10º to 50º (2Θ) using the clay and rock 0.4 program. The XRD was analyzed for the positions of the peaks and crystalline phases for comparing different mixtures.

2.3.3 Fourier Transform Infrared Spectroscopy (FTIR)analysis

The Fourier transform infrared spectrometer model EQUINOX 55 (Bruker) was used to assess the functional groups of the samples. FTIR was performed on the paste samples using the KBr pellet technique over 4000-400 cm^{-1} range.

2.3.4 Scanning electron microscopy (SEM) analysis

For microscopy, small scraps of the samples from the compressive strength tests for 28 days were subjected to scanning electron microscopy. The sectioned portions were first air dried, followed by gold coating for microstructural imaging. A JMS-5800 LV model scanning electron microscope (JEOL, Japan) was used to investigate the microstructure matrix of the mortar samples.

2.3.5 Drying shrinkage test

The change in length of samples was determined with a length comparator. The geopolymer samples were prepared by curing at 80 ºC for 0.5, 1, 2 and 4 h. The first reading was recorded after demolding and then measurements were conducted for each sample every day for the first week, and then once a week for up to 10 weeks.

3. Results and discussion

3.1 The effect of FPRL on compressive strength

The compressive strengths of geopolymer samples, after curing at 80 ºC for 0.5, 1, 2 and 4 h, are shown in Figure 3. The early (immediately after demolding) compressive strength is low but after curing for 4 h it is high, partly because heat curing accelerated geopolymerization forming the mineral phases.

The development of strength of the F (control), 1L, 2.5L and 5L samples heat cured for 0.5, 1, 2 and 4 h is shown in Figure 3a-d, respectively. It can be seen that the compressive strength clearly decreased with FPRL content, due to dilution by water in the FRPL; more FRPL gave higher water content in the geopolymer matrix .Xu et al. [17] and Ben et al. [18] reported that fly ash geopolymer with increased water to solids ratio gave reduced compressive strength. Likewise, when geopolymers were prepared with slag [19], sludge [20] and red mud [21] had high water to powder ratios and reduced the compressive strength. Hawa [22] determined the effects of water to powder ratio on a geopolymer with metakaolin partially replacing oil palm ash. On using water to powder ratios 0.45, 0.55 and 0.65, the results revealed that the lower water to powder ratios gave higher compressive strengths. The geopolymers with heat curing for 0.5, 1 and 2 h kept on developing more strength for up to 28 days. It was observed that samples with 2.5% FPRL and 5% FPRL after 7 days developed only slightly further compressive strength. The compressive strengths remain acceptable also at FRPL contents of 2.5% and 5%. The solids content and water in FPRL partly have opposing effects on the compressive strength. For F-1 (Fig. 3b) case in the present study, the compressive strengths of samples containing only fly ash after 28 days at ambient temperature were highest for the samples cured for only 1 h, which is consistent with the findings of Rovnaník [23].

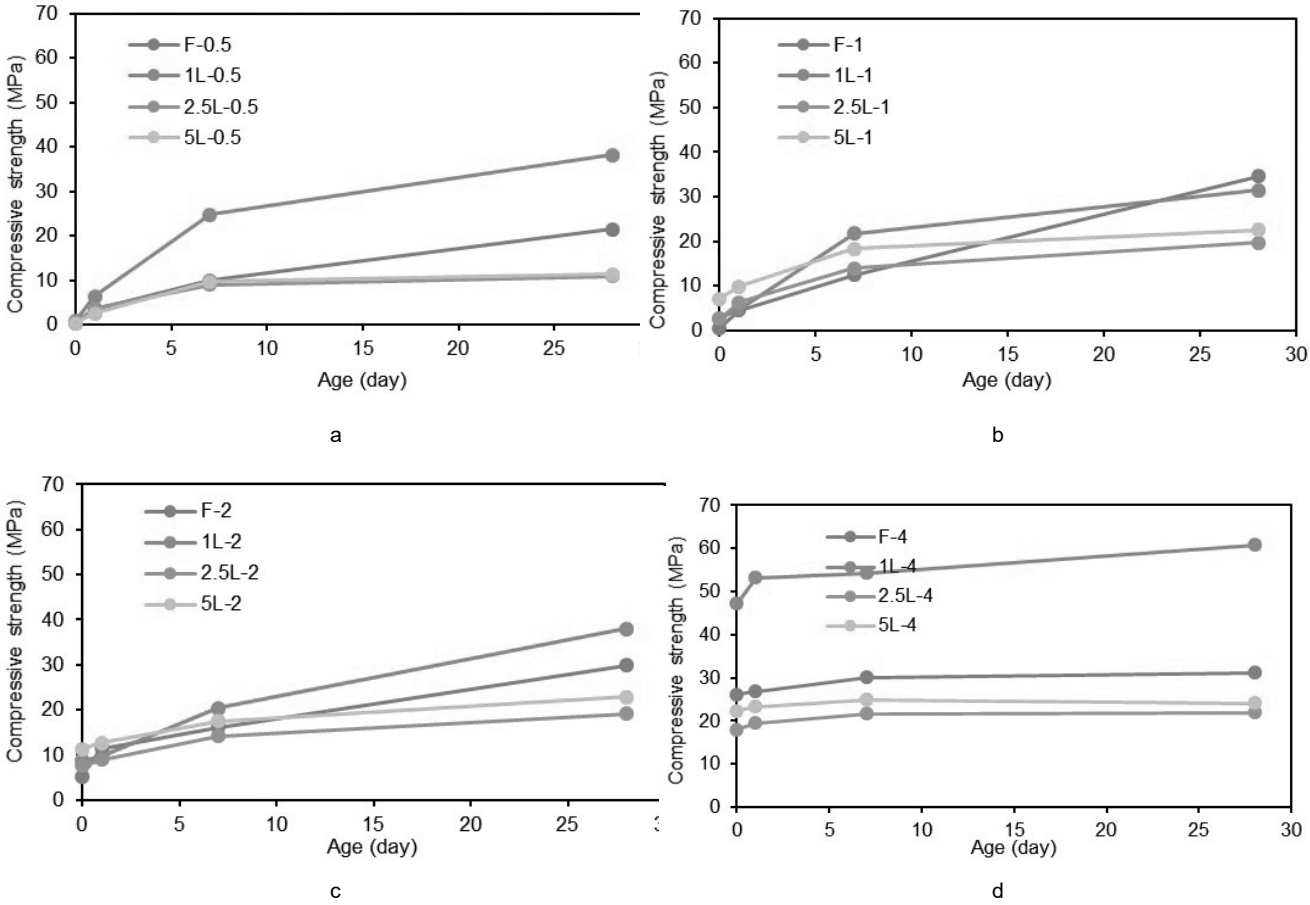

Fig. 3 - Compressive strength of geopolymer mortars with different FPRL contents and heat curing for (a) 0.5 h, (b) 1 h, (c) 2 h, and (d) 4 h.

The compressive strengths of the samples with various amounts of FPRL, heat cured at 80 ºC for 4 h, are shown in Figure 3d. The compressive strength at the age of 28 days is slightly higher the strength after sample curing for 24 hours due to the sample type as high early strength. The longer heat curing clearly accelerated the development of compressive strength at early age. A somewhat similar trend in the compressive strength development was after demolding up to 28 days for F-4, 2. 5L-4 and 5L-4. However, the 1L-4 give the highest compressive strength. This is due to the increased compressive strength was attributable to the structure of the geopolymer samples which had a dense compact matrix and contained less unreacted raw materials. Spherical surfaces of fly ash particles are clearly observed.

3.2 The effects of heat curing on compressive strength

The compressive strengths of geopolymer samples as a function of elevated temperatures curing are illustrated in Figure 4. For all mixtures, longer elevated temperatures curing was found to increase of compressive strength after demolding at ambient temperature, relative to a shorter period of heat curing. Especially heat curing for 4 h gave superior compressive strengths. Longer heat curing may increase the extent of geopolymerization reactions with formation of mineral phases. For 1L sample containing 1% FPRL cured for 0.5, 1, and 2 h, the compressive strengths were quite similar. Aging at ambient temperature did not thereafter generate much difference.

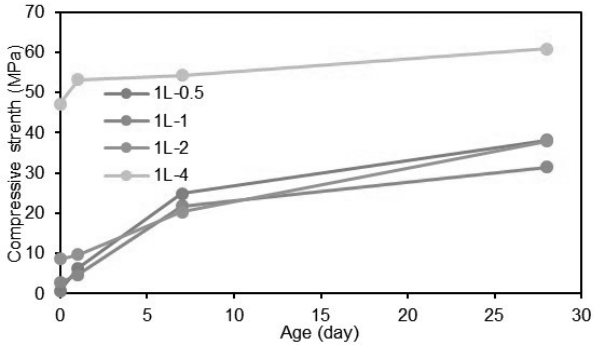

Fig. 4 - Compressive strengths of geopolymer mortars with 1% FPRL.

3.3 Transformation of mineral phases by geopolymerization

The XRD patterns of fly ash based geopolymer containing FPRL and heat cured for 0.5-4 h are shown in Figures 5 and 6. In Figure 5, the mixture binder pastes showed a characteristic

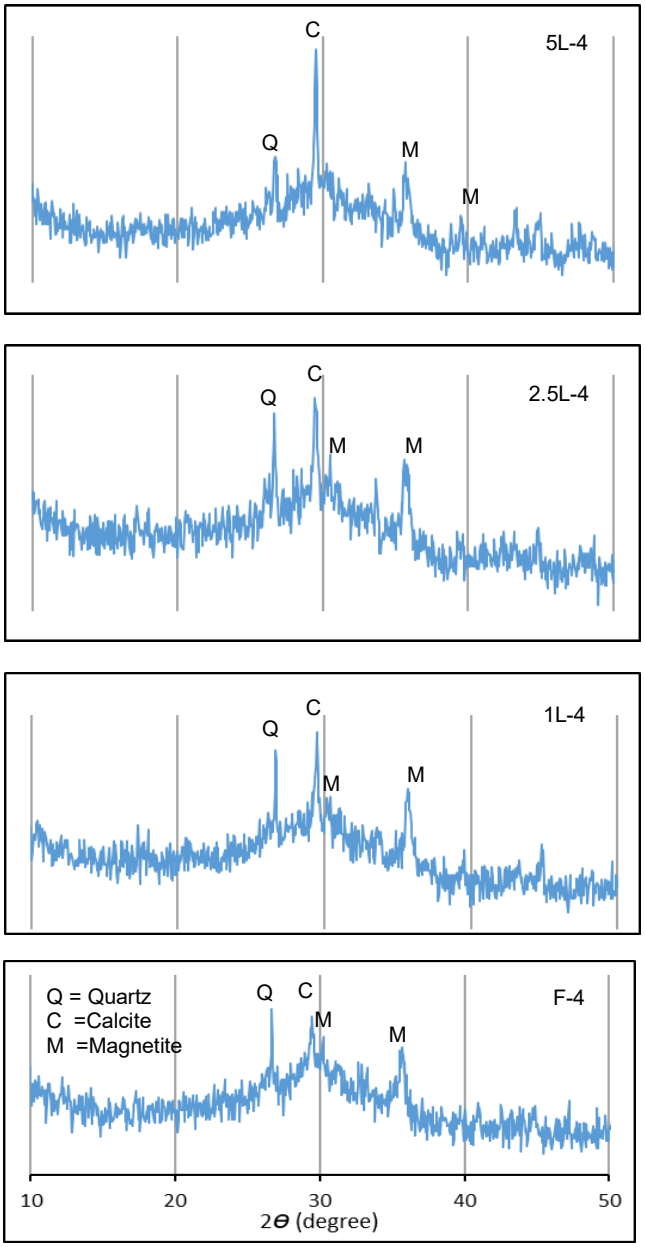

Fig. 5 - XRD patterns of geopolymer binders containing PRL, heat cured for 4-h.

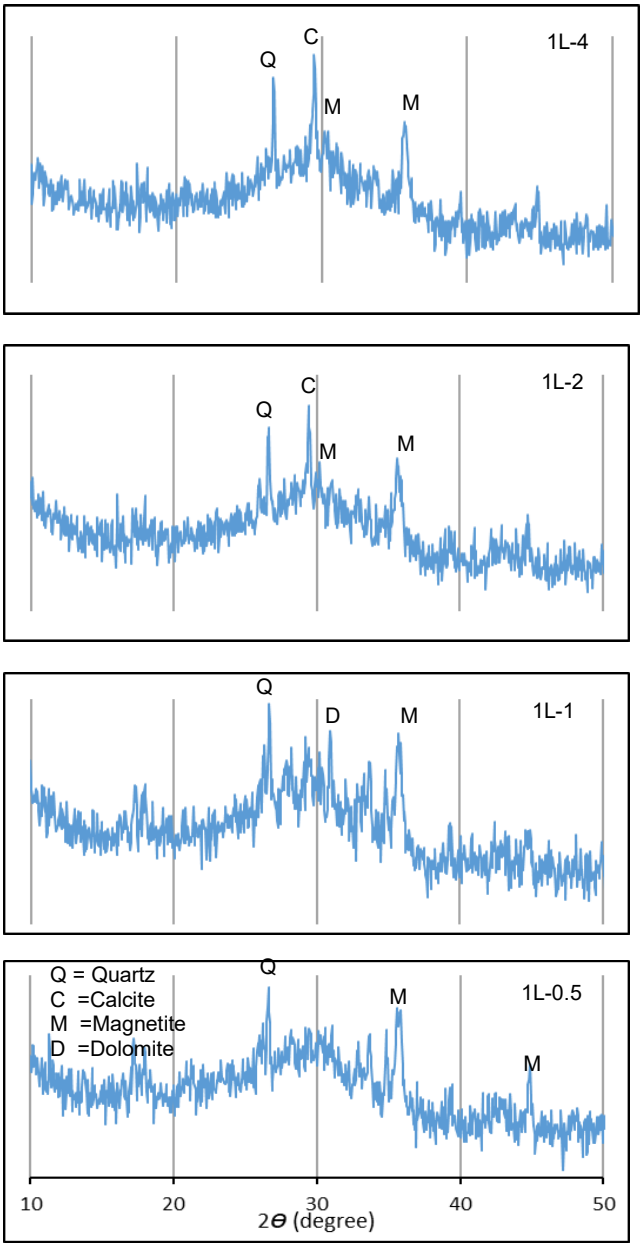

Fig. 6 - XRD patterns of geopolymer binders prepared from 1L, heat cured for 0.5, 1, 2 and 4-h.

high background between 20° and 35° 2θ with shifts increased in the amorphous range between 15° and 35° 2θ (see Fig. 1). The XRD patterns of fly ash had similar test result with a broad hump between 18° and 28° 2θ. It is well known the raw materials were mainly amorphous [24]. On comparing the XRD patterns of fly ash powder in Figure 1 with geopolymer samples in Figure 5, it is observed that some of the strong peaks in fly ash have disappeared, possibly by consumption of the compound in geopolymerization. For example, no geopolymer shows any trace of the crystalline peak at 26° 2θ of fly ash. The geopolymer pastes had similar diffraction patterns as regards the positions of peaks. However, it was observed that the peaks of 1L-4 sample were clearly stronger than for the other samples, differing in FPRL content and heat curing time. The mineralogical characterization of XRD patters showed crystalline and amorphous phases as range between 20° and 35° 2θ. The crystalline phases were prominently shown as magnetite and quartz from fly ash, and the amorphous phase was due to geopolymerization products. The compressive strength of geopolymer samples is highly influenced of aluminosilicate compounds. Consequently, the strong sharp peak of 1L-4 sample matches its high compressive strength (see Fig. 3d).

Figure 6 shows the XRD patterns for samples with 1% FPRL for the heat curing times of 30 min, 1, 2 and 4 h. The four mixtures had similar patterns, mostly amorphous with some crystalline peaks. The sample cured for 4 h showed obvious calcite, quartz and magnetite contents as sharper

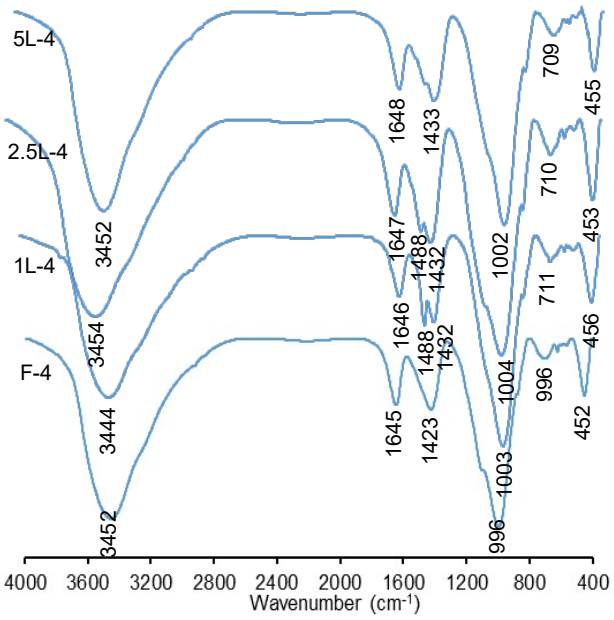

Fig. 7 - FTIR spectra of geopolymers with different %FPRL contents, cured for 4 h.

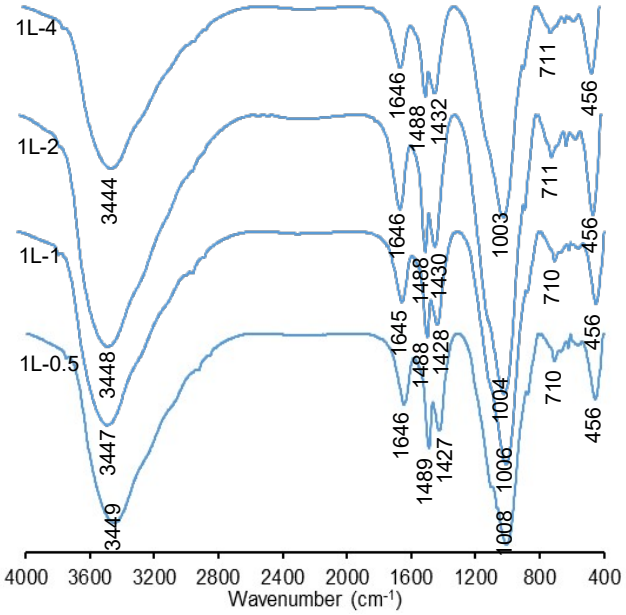

Fig. 8 - FTIR spectra of geopolymers with different heat curing times.

peaks than in the other cases. The longest heat curing produced the strongest peaks and the highest compressive strength. Various studies [25,26] have reported that the XRD patterns indicating high crystallinity are associated with high compressive strength.

3.4 Transformation of FTIR spectra by geopolymerization

A detailed FTIR investigation demonstrated the vibrational transition and changes in peak positions. For understanding of the chemistry of geopolymer pastes, a detailed study of the FTIR was conducted, with consideration of the heat curing times and FPRL contents. As is shown in Figures 7 and 8, some changes can be seen in the range 400-1700 cm^{-1} and approximately at 3500 cm^{-1}. The bands around 450 cm^{-1} represent Si-O bending, and Al-O-Si band is shown around 700 cm^{-1}. Bands at about 1000 cm^{-1} are for Si-O stretching, the vibrations of the CO_3^{2-} groups are at 1430-1480 cm^{-1}, and hydration water (O-H stretching and deformation) bands are centered around 1650 and 3500 cm^{-1}. The main band of geopolymer with fly ash at 1000 cm^{-1} appeared to be sharper in all geopolymer samples. Si-O-Si and Si-O-Al stretching vibrations related to the degree of geopolymerization were noted, with signals around 450 cm^{-1} and 700 cm^{-1}, and the main vibration bands come from interlinked SiO_4 and AlO_4 in tetrahedral configuration [27]. The bands at approximately 450 cm^{-1} are for Si-O vibrations. These major band are near the frequencies reported earlier in the literature for this compound [28]. However, it was observed that the band around 700 cm^{-1} showed new peaks lightly detected in fly ash. Those around 3450 and 1645 cm^{-1} are for the O-H stretching vibrations and the H-O-H bending vibrations, respectively. This has been reported earlier for hydroxyl groups [29]. The presence of sodium carbonate is indicated by the band near 1430 cm^{-1}, the carbonate peak appears when the solid polymer is dried after curing [30], while the carbonate in geopolymer matrix is seen at approximately 1490 cm^{-1}. However, some studies [31] have reported that bands in the 1430 and 1490 cm^{-1} region for a geopolymer matrix are attributed to the stretching of CO_3^{2-} groups. These bands are generated by CO_2 from the air participating in geopolymerization reactions.

The major peak in geopolymer binder system is the vibration band around 1000 cm^{-1} and is attributed to asymmetric stretching of Si-O-T (Si or Al) bonds in the geopolymerization products. A shift of this band to lower wave numbers can be seen in fly ash and geopolymer. It is indicative of the formation of a aluminosilicate gel [28]. However, the investigation suggests that aluminosilicate formed in geopolymer of fly ash containing FPRL and alkaline activator gives a slightly different FTIR pattern. The effects of FPRL content and heat curing time on the microstructure are shown in Figures 7 and 8, and are rather limited. A prior study [32] reported that the FTIR spectra of fly ash based geopolymer with different water-to-binder ratios had limited variations in the gel microstructure. In our ongoing study, the quantitative XRD and microstructural images can better match the observed strengths than the FTIR spectra.

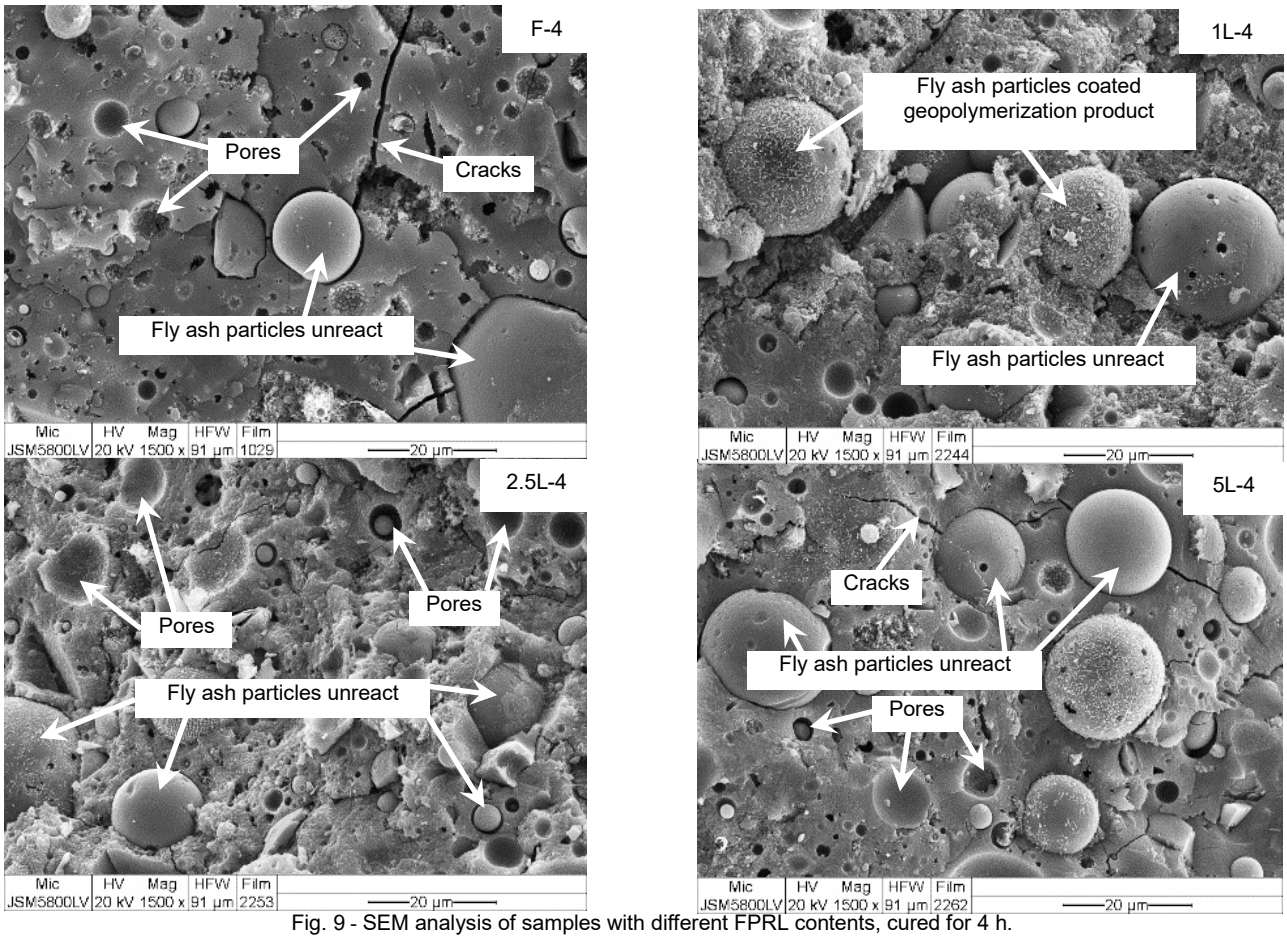

Fig. 9 - SEM analysis of samples with different FPRL contents, cured for 4 h.

3.5 Morphological and microstructural analysis of geopolymer binder

Microstructural evolution of the geopolymer binders was monitored using scanning electron microscopy. Figure 9 shows representative images of geopolymerization product morphology. The binder structure shows small pores in all areas. The globules observed in the system are on the order of a micron in diameter, but the globular structures are not connected in a network. In the micrographs, it can be observed that the samples are porous in nature and the particles are globular in shape. The globular particles seen in the SEM images were silica. Particles that appear flat are primarily silica from the fly ash. The F-4, 2. 5L-4 and 5L-4 samples shown clearly unreacted raw material. No geopolymerization products appear on the silica globular surfaces, and it was observed that an interfacial transition zone between the globular surface and matrix had lacuna around the silica particles. However, 1L-4 sample shows geopolymerization products on silica particles surface. The SEM images showed that a homogenous microstructure, continuous matrix with silica particles and pores were found. The fly ash particles were combined by the cementitious reactions that provided a dense, compact microstructure, which explains high compressive strength (see Fig. 3d). In a similar study on geopolymer with fly ash cured at ambient temperature, Somna et al. [33] showed that fly ash particles in geopolymer matrix were coated with geopolymerization products serving as nucleation sites for further processes.

Regarding the different heat curing times as shown in Figure 10, for 1L-4 the microstructure was quite much more homogeneous than in geopolymer samples heat cured for 0.5, 1 and 2 h. Too short heat curing left unreacted fly ash particles unutilized during geopolymerization. An interlocking network between globular surfaces of fly ash and matrix is observed, which provided compressive strength to the geopolymer. Hawa et al. [34] have shown that in geopolymers heat cured for 1-4 h, the long heat curing gave a dense compact microstructure and lower proportion of unreacted raw material. This is consistent with the higher compressive strength.

3.6 Drying shrinkage

The drying shrinkages of the geopolymer mortars are shown in Figures 11 and 12. The samples differ in FPRL contents and in heat curing times, and the monitoring was continued for up to 70 days. It was observed that shrinkage of geopolymer mortars with longer heat curing times decreased but short heat curing provided rapid shrinkage up to 7 days. For example, in Figure 11 the geopolymer samples cured for 0. 5 h (30 min) were stabilized after 21 days, whereas samples

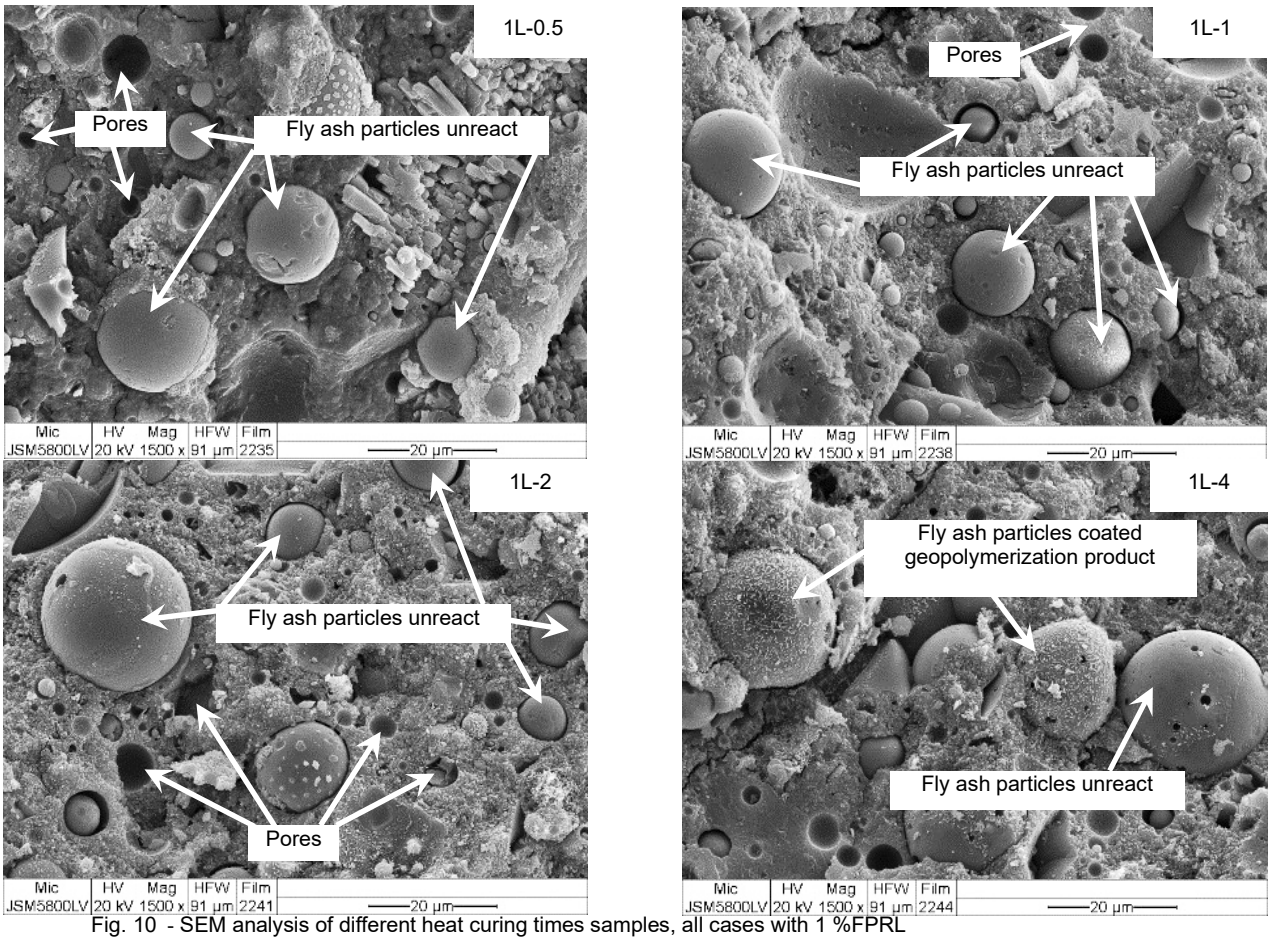

Fig. 10 - SEM analysis of different heat curing times samples, all cases with 1 %FPRL

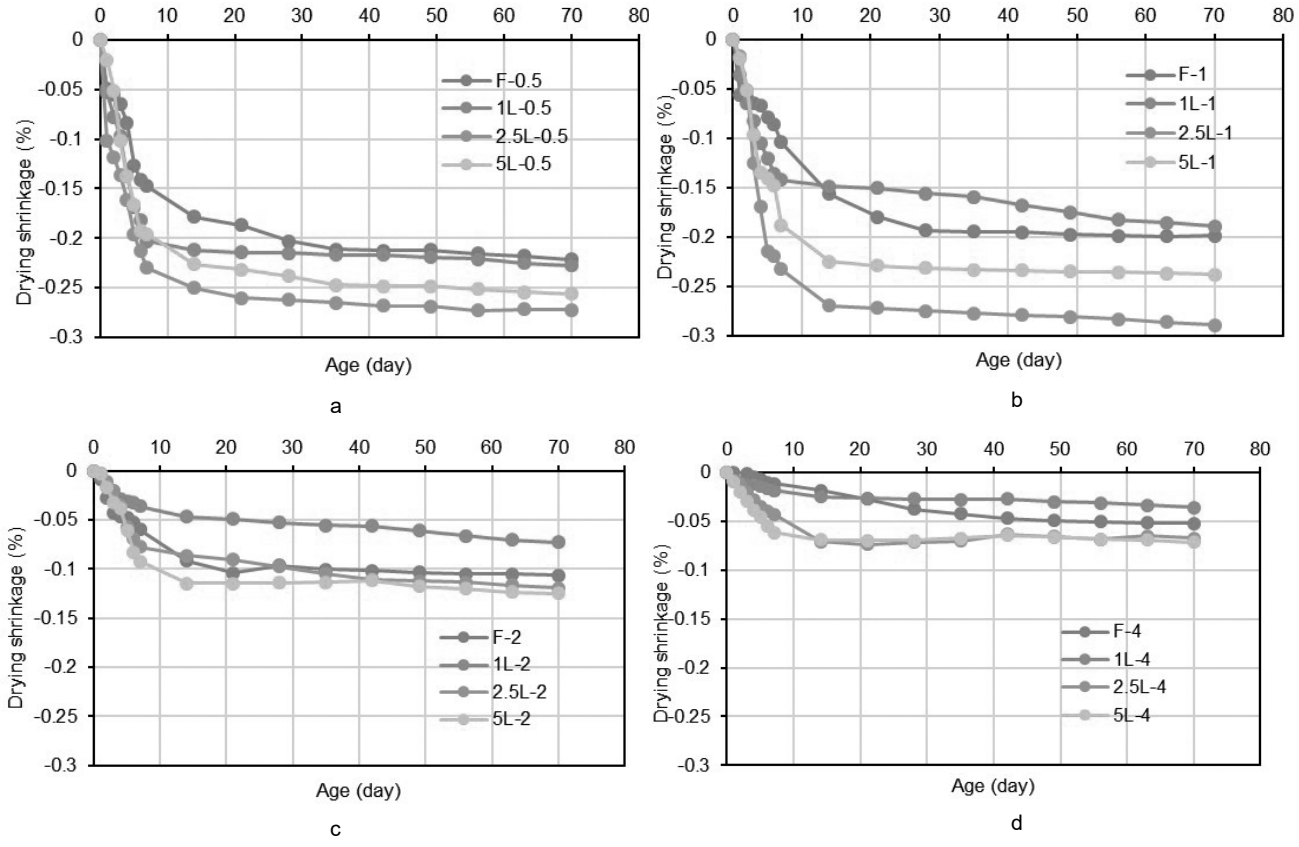

Fig. 11 - Drying shrinkages of geopolymer mortars cured for (a) 0.5 h, (b) 1 h, (c) 2 h and (d) 4 h.

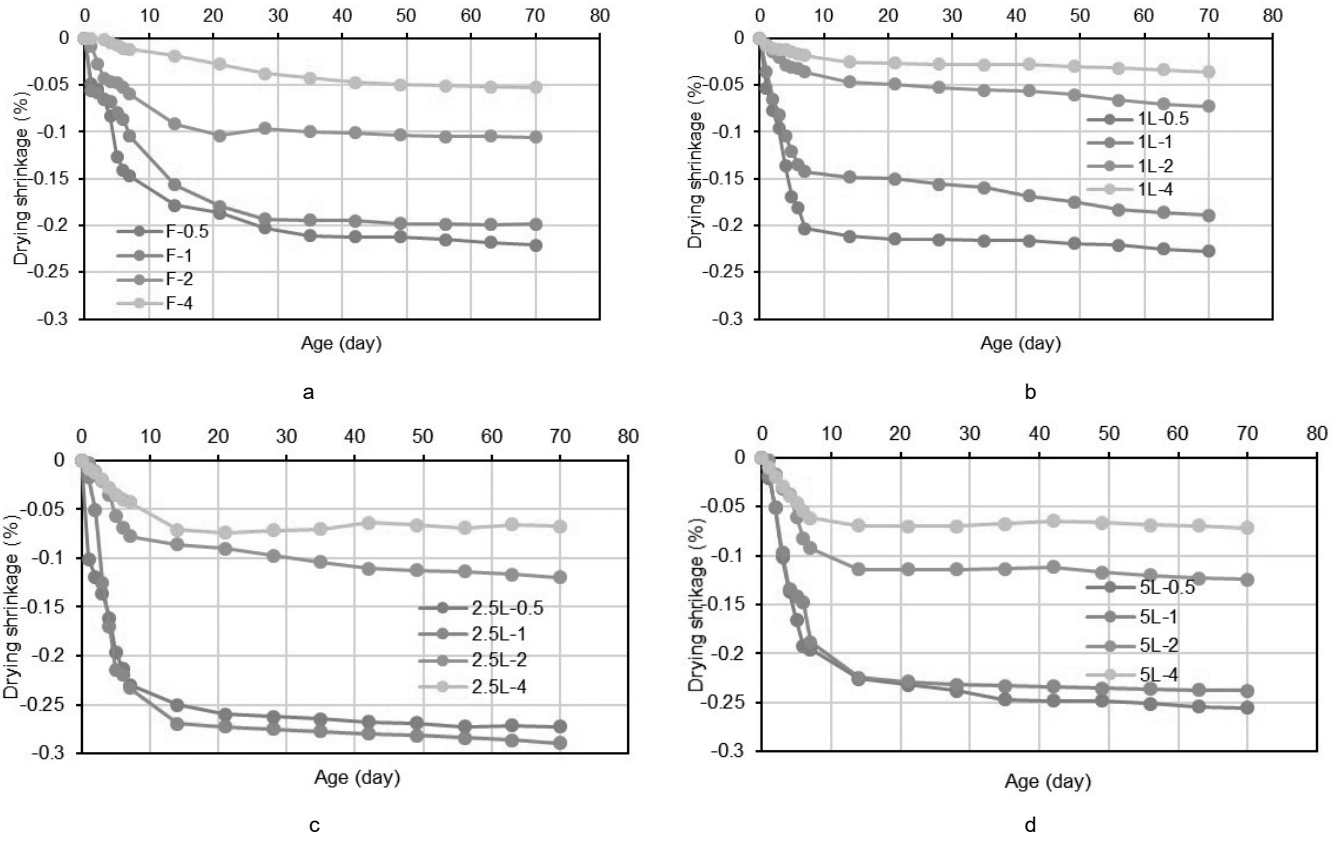

Fig. 12 - Drying shrinkages of geopolymer mortars containing FPRL: (a) 0%, (b) 1%, (c) 2.5%, and (d) 5%.

cured for 2 h stabilized after 14 days. This is because a longer heat curing requires more water to be used in geopolymerization. Thus, after taking off the polyvinyl cover and demolding, a high volume of free water in the pores of matrix took a long time to evaporate. For the samples with various FPRL content, the shrinkage increased with FPRL content. This is because of the water in FPRL, influences high free water to the geopolymer mixes.

In Figure 12, the drying shrinkages are shown for samples containing 0%, 1%, 2.5% and 5% FPRL, heat cured at 80 ºC for 0.5, 1, 2 and 4 h. The longer heat curing times decreased the shrinkage. For example, the 1L sample (Fig.12b) cured for 0. 5 and 1 h had similar shrinkage behavior, especially, early age tests sample. It was observed that the drying shrinkage in the first 7 days for the geopolymers cured for 0. 5 and 1 h were closely similar, and after that decreased. On the other hand, the samples cured for 2 and 4 h had consistently lesser drying shrinkage than those cured for 0.5 and 1 h. This was because the longer heat curing caused loss of water by both evaporation and by geopolymerization reactions.

4. Conclusions

Geopolymers prepared with fly ash and small amounts of FPRL were synthesized and studied. The duration of heat curing affected compressive strength, drying shrinkage, and the microstructure. The following conclusions can be drawn from the investigation and test results.

- Heat curing for 4 h determined high early compressive strength, especially for the sample with 1% FPRL (1L-4) with a slight increase in compressive strength by curing in normal conditions for up to 28 days.
- The highest compressive strengths were developed by geopolymer mortars containing 1% FPRL for any of the tested curing times, and among these the highest for 4 h of curing.
- SEM images demonstrate the good reaction extent in 1L-4 sample with low presence of unreacted fly ash particles.
- The lowest drying shrinkage was obtained with 1% FPRL for all heat curing times.
- Longer curing at elevated temperature also decreased drying shrinkage, likely by reducing the free water content remaining after curing.
- Heat curing for 4 h assured good engineering properties in terms of both compressive strength and drying shrinkage.

Geopolymer mortars prepared from fly ash with added FPRL can be used as structural materials. Especially they appear appropriate for repair of concrete substrates such as concrete pavement. On the other hand, mixes with high FPRL content can be used to manufacture of concrete blocks, bricks, and panel walls.

Acknowledgements

The authors gratefully acknowledge the financial support from the National Research Council of Thailand and TRF Senior Research Scholar (RTA62), as well as the use of facilities of the Infrastructure and Materials Innovation Research Unit and Department of Civil Engineering, Princess of Naradhiwas University, Amphur Muang, Narathiwat, The authors would like to give a special thanks Assoc. Prof. Seppo Karrila, Prince of Songkla University for improving the English of this article.

REFERENCES

[1] N. Ranjbar,M. Mehrali, U.J. Alengaram, H.S.C. Metselaar, and M.Z. Jumaat, Compressive strength and microstructural analysis of fly ash/ palm oil fuel ash based geopolymer mortar under elevated temperatures, Construction and Building Materials, 2014, **65**, 114-121.

[2] N. Ranjbar, M. Mehrali, A. Behnia, U.J. Alengaram, M.Z. Jumaat, Compressive strength and microstructural analysis of fly ash/palm oil fuel ash based geopolymer mortar, Construction and Building Materials, 2014, **59**, 532-539.

[3] S. Songpiriyakij, T. Kubprasit,C. Jaturapitakkul, and P. Chindaprasirt, Compressive strength and degree of reaction of biomass -and fly ash-based geopolymer, Construction and Building Materials, 2010, **24**, 236-240.

[4] H. Zhu, G. Liang, J. Xu, Q. Wu, and M. Zhai, Influence of rice husk ash on the waterproof properties of ultrafine fly ash based geopolymer, Construction and Building Materials, 2019, **208**, 294-401.

[5] J. Xie, J. Wang, R. Rao, C. Wang, and C. Fang, Effects of combined usage of GGBS and fly ash on workability and mechanical properties of alkali activated geopolymer concrete with recycled aggregate, Composites Part B :Engineering, 2019, **164**, 179-190.

[6] A. Bouaissi, L.Y. Li, M.M. Al Bakri Abdullah, and Q.B. Bui, Mechanical properties and microstructure analysis of FA-GGBS-HMNS based geopolymer concrete, Construction and Building Materials, 2019, **210**, 198-209.

[7] T. Alomayri, Experimental study of the microstructural and mechanical properties of geopolymer paste with nano material (Al_2O_3), Journal of Building Engineering, 2019, **25**, 100788.

[8] F.N. Okoye, J. Durgaprasad, N.B. Singh, Effect of silica fume on the mechanical properties of fly ash based-geopolymer concrete, Ceramics International, 2016, **42**(2), Part B, 3000-3006.

[9] A. Badanoiu, E. Iordache, R. Ionescu, G. Voicu, E. Matei, Effect of composition and curing regime on some properties of geopolymers based on cathode ray tubes glass waste and fly ash, Romanian Journal of Materials, 2015,**45**(1), 3-13.

[10] C.L. Hwang and T.P. Huyunh, Effect of alkali-activator and rice husk ash content on strength development of fly ash and residual rice husk ash-based geopolymers, Construction and Building Materials, 2015, **101**, 1-9.

[11] M.Y.J. Liu, C.P. Chua, U.J. Alengaram, and M.Z. Jumaat Utilization of palm oil fuel ash as binder in lightweight oil palm shell geopolymer concrete, Advance in Materials Science and Engineering, 2014, 6 . http//:dx.doi.org/10.1155/2014/610274

[12] J. Temuujin, A. van Riessen, and R. Williams, Influence of calcium compounds on the mechanical properties of fly ash geopolymer pastes, Journal of Hazardous Materials, 2009, **167**, 82-88.

[13] P. Chindaprasirt, P. Paisitsrisawat, and U. Rattanasak, Strength and resistance to sulfate and sulfuric acid of ground fluidized bed combustion fly ash-silica fume alkali-Activated composite, Advanced Powder Technology, 2014, **25**(3), 1087-1093.

[14] A. Hawa, P. Salaemae, W. Prachasaree, and D. Tonnayopas, Compressive strength and microstructural charateristics of fly ash based geopolymer with high volume field Para rubber latex, Romanian Journal of Materials, 2017, **47**(4), 462-469.

[15] The Thai Rubber Association, www.thainr.com/uploadfile/ 20190124135406.pdf

[16] ASTM C109/ C109M-16, Standard Test Method for Compressive Strength of Hydraulic Cement Mortars (Using 2-in. or [50-mm] Cube Specimens), ASTM International, West Conshohocken, PA, USA, 2016.

[17] F. Xu, X. Deng, C. Peng, J. Zhu, and J. Chen, Mix design and flexural toughness of PVA fiber reinforced fly ashgeopolymer composites, Construction and Building Materials, 2017, **150**, 179-189.

[18] C.C. Ban, P.W. Ken, and M. Ramli, The hybridizations of coal fly ash and wood ash for the fabrication of low alkalinity geopolymer load bearing block cured at ambient temperature, Construction and Building Materials, 2015, **88**, 41-55.

[19] K.H. Yang, C.W. Lo, and J.S. Huang, Production and properties of foamed reservoir sludge inorganic polymers, Cement and Concrete Composite, 2013, 38, 50-56.

[20] J.H. Chen, J.S. Huang, and Y.W. Chang, Use of reservoir sludge as a partial replacement of metakaolin in the production of geopolymers, Cement and Concrete Composite, 2011, **33**(5), 602-610.

[21] N. Ye, J. Yang, S. Liang, Y. Hu, J. Hu, B. Xiao, and Q. Huang, Synthesis and strength optimization of one-part geopolymer based on red mud, Construction and Building Materials, 2016, **111**, 317-325.

[22] A. Hawa, W. Prachasaree, and D. Tonnayopas, Effect of water-to-powder ratios on the compressive strength and microstructure of metakaolin based geopolymers, Indian Journal of Engineering and Materials Sciences, 2017, **24**(6), 499-506.

[23] P. Rovnaník, Effect of curing temperature on the development of hard structure of metakaolin-based geopolymer, Construction and Building Materials, 2010, **24**(7), 1176–1183.

[24] M.Z. Nazir Khan, F.A. Shaikh, Y. Hao, and H. Hao, Synthesis of high strength ambient cured geopolymer composite by using low calcium fly ash, Construction and Building Materials, 2016, **125**, 809-820.

[25] E. Alvarez-Ayuso, X. Querol, F. Plana et al., Environmental, physical and structural characterisation of geopolymer matrixes synthesised from coal (co-) combustion fly ashes, Journal of Hazardous Materials, 2008, **154**(1-3), 175–183.

[26] A. M. M. Al Bakri, H. Kamarudin, M. Bnhussian, A. R. Rafza, and Y. Zarina, Effect of Na_2SiO_3/ NaOH ratios and NaOH molarities on compressive strength of fly ash-based geopolymer, ACI Materials Journal, 2012, **109**(48), 503–508.

[27] A. Fernandez-Jimenez, A. Palomo, T. Vazquez, R. Vallepu, T. Terai, and K. Ikeda, Alkaline activation of blends of metakaolin and calcium aluminate, Journal of American Ceramics Society, 2008, **91**(4), 1231–1236.

[28] M. Criado, A. Fernandez-Jimenez, and A. Palomo, Alkali activation of fly ash . Part III : effect of curing conditions on reaction and its graphical description, Fuel, 2010, **89**(11), 3185–3192.

[29] P. Chindaprasirt, C. Jaturapitakkul, W. Chalee, and U. Rattanasak, Comparative study on the characteristics of fly ash and bottom ash geopolymers, Waste Management, 2009, **29**, 539-543.

[30] V. Barbosa, K. MacKenzie, and C. Thaumaturgo, Synthesis and characterisation of materials based on inorganic polymers of alumina and silica : sodium polysialate polymer . International Journal of Inorganic Materials, 2000, **2**(4), 309–317.

[31] Z. Sun and A. Vollpracht, One year geopolymerisation of sodium silicate activated fly ash and metakaolin geopolymers, Cement and Concrete Composite, 2019, **95**, 98-110.

[32] I. Ismail, S. A. Bernal, J. L. Provis, S. Hamdan, and J. S. J. van Deventer, Microstructural changes in alkali activated fly ash/ slag geopolymers with sulfate exposure, Materials and Structure, 2013, **46**(3), 361–373.

[33] K. Somna, C. Jaturapitakkul, P. Kajitvichyanukul, and P. Chindaprasirt, NaOH-activated ground fly ash geopolymer cured at ambient temperature, Fuel, 2011, **90**(6), 2118–2124.

[34] A. Hawa, D. Tonnayopas, and W. Prachasaree, Performance Evaluation and Microstructure Characterization of Metakaolin-Based Geopolymer Containing Oil Palm Ash, The Scientific World Journal, 2013, dx.doi.org/10.1155/2013/857586.

****